J Biol Phys (2009) 35:361–382
DOI 10.1007/s10867-009-9143-2

ORIGINAL PAPER

Dynamics of a minimal neural model consisting of an astrocyte, a neuron, and an interneuron

Angelo Di Garbo

Received: 28 November 2008 / Accepted: 16 February 2009 /
Published online: 7 May 2009
© Springer Science + Business Media B.V. 2009

Abstract In this paper, a biophysical neural network model consisting of a pyramidal neuron, an interneuron, and the astrocyte is studied. The corresponding dynamical properties are mainly investigated by using numerical simulations. The results show that the presence of the adenosine triphosphate and of the interneuron impacts the overall neural activity. It is shown that the fluxes of calcium through the cellular membrane strongly affect the modulation of the neural activity arising from the astrocyte.

Keywords Neuron · Interneuron · Astrocyte · Receptors · Glutamate · ATP · Calcium

1 Introduction

In the nervous system of vertebrates, there are more glial cells than neurons: from ten to 50 times, depending on the animal type. What are glial cells and which is their functional role? Glial cells are not able to generate action potentials but, nevertheless, they play an important role for the functioning of the brain's different areas. There are two classes of glial cells: the microglia and the macroglia. The cells belonging to the microglia class play an important role in protecting the brain against infections: they are capable of phagocytosis that protects the neurons of the central nervous system. In the central nervous system, the more important cells belonging to the macroglia class are the astrocytes and the oligodendrocytes. The astrocytes are the more abundant cell type and they are connected by gap junctions, thus forming a large functional syncytium. Astrocytes, through their processes, are close to synapses and to the vasculature. Experimental evidence has shown that there is a bi-directional intercommunication between the vascular system and the astrocyte [1]. The astrocyte processes close to synapses have a high density of neurotransmitter receptors that are used to get information on the level of synaptic activity. One important task of the

A. Di Garbo (✉)
Istituto di Biofisica CNR, Via G. Moruzzi 1, 56124, Pisa, Italy
e-mail: angelo.digarbo@pi.ibf.cnr.it

astrocyte is to clean the extracellular space when high concentrations of neurotransmitters and ions are present [2]. Of particular relevance is the control of the concentration of the extracellular potassium that, at high concentration, can promote epileptic phenomena [2]. Lastly, astrocytes contribute to neural metabolism by furnishing glucose to neurons [2]. The oligodendrocytes play an important role in neural intercommunication by providing myelin to neurons to cover axons, which allows electrical signals to propagate faster [2].

A wide variety of neurotransmitter receptors are expressed in the astrocytic plasma membrane and experimental findings reveal that astrocytes located near synapses respond to neurotransmitters (including glutamate, gamma-aminobutyric acid, adenosine triphosphate (ATP), etc.) with an elevation of their intracellular calcium levels ($[Ca^{2+}]_i$) [3–14]. The $[Ca^{2+}]_i$ increase in these cells mediates the release of glutamate, ATP, and other neuroactive substances that are capable, by a feedback mechanism, of modulating synaptic communication between neurons [11–14]. In addition, a calcium-independent pathway of glutamate release from astrocytes also occurs, through the activation of the $P2X_7$ receptor [15]. In the nervous system, ATP is an important extracellular messenger and its action on astrocytes is mediated by ionotropic (P2X) and metabotropic (P2Y) purinoreceptors [14, 16]. Experimental evidence indicates that in the synaptic cleft the presence of extracellular ATP contributes to synaptic transmission by activating postsynaptic P2X receptors [17–19].

In the present paper, the effects on the neural dynamics of the reciprocal intercommunication between neuron, interneuron, and astrocyte will be investigated by using a biophysical modeling approach.

2 Computational models

2.1 The mechanisms underlying astrocyte excitability

The stimulation of an astrocyte with a depolarizing current determines a membrane depolarization of the cell. However, the low density of sodium channels on the cell membrane does not permit the generation of an action potential. Therefore, astrocytes are a typical example of nonexcitable cells. Do astrocytes have another kind of excitability? The response is yes and will be briefly described qualitatively in what follows. First of all, let us ask whether astrocytes are capable of listening to the ongoing synaptic communication between neurons. The results of crucial experiments have shown that the presence of glutamate in proximity of astrocytes determines a transient elevation of the concentration of the intracellular calcium in these cells [5, 20]. In some cases, calcium waves and oscillations were also observed [21]. These experiments imply that glutamate receptors are expressed in the astrocyte membrane. Successive experiments, carried out during the past decade, confirmed these results; consequently, the notion that the transient elevation of the intracellular calcium level in astrocytes represents a form of excitability of these cells is now widely accepted. Nowadays, it is known that there are a large number of receptors on the cellular membrane of astrocytes (both ionotropic and metabotropic) and that these cells use them to obtain biochemical information about the extracellular medium. The results of several experiments have shown that the activation of these receptors determines a transient elevation of the intracellular calcium level in the astrocytes [1, 11, 22, 23]. For instance, the presence of extracellular ATP determines the activation of ionotropic (P2X) and metabotropic (P2Y) purinergic receptors, both leading to the transient elevation of the

intracellular calcium level in the astrocytes. Overall, given that glutamate and ATP are released during synaptic activity, the phenomena described above suggest that astrocytes listen to the level of synaptic activity and then respond by transient elevations of their cytoplasmic calcium level.

2.2 Astrocytes modulate neural activity

As discussed before, the activation of astrocytes leads to the release of neurotransmitters by these cells (gliotransmission). The consequence of this phenomenon is a modulation of the synapses that are close to the astrocyte processes. Thus, these experimental results are at the basis of the concept of the tripartite synapse, consisting of the presynaptic neuron, the postsynaptic neuron, and the astrocyte. The main neurotransmitters that are released by astrocytes are glutamate and ATP, and in what follows their release and modulation properties will be briefly described. Thanks to important experimental studies, it was shown that glutamate is released by these cells with mechanisms similar to that regulating its release from the presynaptic terminal [24–29]. The glutamate released from astrocytes can act on the presynaptic neuron by modulating its synaptic activity, or on the postsynaptic neuron by determining its depolarization. Modulation of synaptic activity is mediated by the activation of the metabotropic and kainate receptors of the presynaptic neuron. The preponderant effect of this event consists in the strengthening of the synapse that arises from an increase of the fusion probability of the vesicles containing the neurotransmitter [1, 11, 23]. The depolarization of the postsynaptic neuron arising from the glutamate released from the astrocyte is mediated by the extrasynaptic *N*-methyl-D-aspartate (NMDA) receptors [30–33]. In fact, by means of simultaneous recordings of the electric activity of the neuron and of the intracellular calcium level of the astrocyte, it was shown that the release of glutamate from astrocytes is followed by the depolarization of the neuron [8]. The depolarization current is characterized by slow kinetics: the rise time constant (τ_R) is of the order of 60 ms and the decay time constant (τ_D) is about 600 ms. This current is much slower than that arising from the activation of the synaptic NMDA receptors: $\tau_R \sim 10$ ms, $\tau_D \sim 150$ ms. Which is the functional role of the release of glutamate from astrocytes? The results of a series of important experiments suggest that the glutamate released by the astrocytes can promote neural synchronization [31, 32]. It is important to stress this last point for its possible implications on the mechanisms underlying the generation of epileptic events. In fact, a deeper knowledge about the effects on neural activity of glutamate released from the astrocytes should be important in the search for new and more efficient methods to control the high synchronization level occurring during epileptic phenomena.

As mentioned above, ATP is also released from astrocytes in a calcium-dependent manner, although the precise mechanisms driving its release are not completely understood [1, 16]. Recent studies have pointed out that ATP can be released by astrocytes by different biochemical mechanisms, including those involving the fusion of vesicles containing ATP with the cellular membrane [16]. In a neural population, the release of ATP from astrocytes determines a modulation of synaptic transmission. For instance, it was shown that in the retina the activation of astrocytes and of the glial Muller cells leads to the release of ATP in the extracellular medium. Then, the ATP is degraded to adenosine which, in turn, by activating the presynaptic A1 receptors, mediates a suppression of synaptic transmission [34, 35]. Moreover, it was shown that in hippocampal preparations the release of ATP by astrocytes determines a reduction of excitatory synaptic transmission [1, 11, 23]. In this

last case, the modulatory effects of ATP occur by two distinct mechanisms: by adenosine acting on the presynaptic A1 receptors and by the activation of presynaptic purinergic receptors.

2.3 Biophysical model of calcium signaling in astrocytes

The model describing calcium dynamics adopted in this paper is that of Di Garbo et al. [36]. In this model, the calcium fluxes through the membrane are the following: (1) a leakage Ca^{2+} influx described by the rate ν_{LM}; (2) a capacitive calcium entry (CCE) of rate ν_{CCE}; (3) an extrusion across the plasma membrane described by the rate ν_{OUT}; (4) an influx of Ca^{2+} mediated by the P2X ionotropic ATP receptor with rate $\nu_{ATP(P2X)}$. Following Höfer et al. [37], two different biochemical processes mediating the production of IP_3 are included: PLCβ and PLCδ. The first one is responsible for the production of IP_3 in the presence of extracellular agonists and is activated through a G-protein-coupled receptor mechanism with rate $\nu_{PLC\beta}$; the second one describes the production of IP_3 arising from the $[Ca^{2+}]_i$ increase, and the corresponding rate is $\nu_{PLC\delta}$. The degradation of the IP_3 is described by the rate $\nu_{IP3(Deg)}$. The binding of the IP_3 molecules to the corresponding receptors on the endoplasmic reticulum (ER) compartment leads to the release of calcium from the ER stores with rate $\nu_{ER(Rel)}$. The free cytosolic calcium is pumped into the ER with a rate ν_{SERCA}. The active fraction of IP_3 receptors on the ER membrane determines the IP_3-induced release of calcium from the ER stores and the time evolution of the concentration of these receptors is described by the two rates $\nu_{IP3R(Rec)}$ and $\nu_{IP3R(Inact)}$.

Let Ca_i denote the concentration of calcium in the cytoplasm of the astrocyte (in micromolar units); Ca_{ER} is the concentration (μM) of calcium in the ER stores; I is the concentration (μM) of IP_3; R the fraction of active IP_3 receptors on the ER membrane. Then, the set of balance equations describing the time evolution of these variables is:

$$dCa_i/dt = \nu_{LM} + \nu_{CCE} + \nu_{ATP(P2X)} - \nu_{OUT} + \nu_{ER(Rel)} - \nu_{SERCA} \tag{1a}$$

$$dCa_{ER}/dt = \beta(\nu_{SERCA} - \nu_{ER(Rel)}) \tag{1b}$$

$$dR/dt = \nu_{IP3R(Rec)} - \nu_{IP3R(Inact)} \tag{1c}$$

$$dI/dt = \nu_{PLC\beta} + \nu_{PLC\delta} - \nu_{IP3(Deg).} \tag{1d}$$

The values of the corresponding constants are reported in Table 1. One of the most commonly observed mechanisms of driven calcium entry from the plasma membrane in nonexcitable cells, like astrocytes, is the CCE [38, 39]. By analogy with a capacitor, the depletion of intracellular stores activates a signaling process leading to the opening of a plasma membrane channel through which calcium enters into the cell. Several theories have been proposed to explain the communication mechanisms between stores and plasma membrane CCE channels. In general, two main experimental models of channel opening have been proposed: one is based on the hypothesis of a small diffusible messenger released from the depleted ER [40] and the second suggests a direct or indirect physical contact between ER proteins and the plasma membrane [41]. In the model used here, this calcium entry pathway is modeled as a nonlinear function of C_{ER}:

$$\nu_{CCE} = k_{CCE}\, H_{CCE}^2 / \left(H_{CCE}^2 + Ca_{ER}^2\right). \tag{2}$$

Table 1 Values of the constants

Description	Symbol	Value
Rate of calcium leak across the plasma membrane	k_0	0.03 μM s^{-1}
Rate of calcium leak from the ER	k_1	0.0004 s^{-1}
Rate of calcium release through IP_3 receptor	k_2	0.2 s^{-1}
Rate constant of SERCA pump	k_3	0.5 s^{-1}
Rate of calcium extrusion from plasma membrane	k_5	0.5 s^{-1}
Rate constant of IP_3 receptor inactivation	k_6	4 s^{-1}
Rate constant of IP_3 receptor degradation	k_9	0.08 s^{-1}
Rate constant of PLCδ	v_7	0.02 μM s^{-1}
Half saturation constant for IP_3 activation of the corresponding receptor	K_{ip3}	0.3 μM
Half saturation constant for calcium activation of the IP_3 receptor	K_a	0.2 μM
Half saturation constant for calcium inhibition of the IP_3 receptor	K_i	0.2 μM
Half saturation constant for calcium activation of PLCδ	K_{Ca}	0.3 μM
Ratio of the effective volumes for calcium of cytoplasm and ER	β	35
Half inactivation constant for CCE influx	H_{CCE}	10 μM
Maximal rate constant for CCE influx	k_{CCE}	0.01 μM s^{-1}
Maximal rate of ATP-evoked ionotropic calcium influx	$k_{ATP(P2X)}$	0.08 μM s^{-1}
Half saturation constant for ATP-evoked ionotropic calcium influx amplitude	$H_{ATP(P2X)}$	0.9 μM
Maximal rate of IP_3production mediated by the metabotropic ATP receptor	$k_{ATP(P2Y)}$	0.5 μM s^{-1}
Dissociation constant for the binding of ATP to the P2Y receptor	K_D	10 μM

The adopted values of the constants k_{CCE} and H_{CCE} were chosen to mimic, at best, the experimental features of the calcium response of an astrocyte in the presence of extracellular ATP [36].

Astrocytes express a wide variety of neurotransmitter receptors that, when activated by appropriate agonists, evoke a large repertory of responses, including $[Ca^{2+}]_i$ increase and release of gliotransmitters like glutamate and ATP [11–14, 34, 35, 42]. ATP participates in calcium signaling by acting on purinergic receptors P2X (ionotropic) and P2Y (metabotropic) [14, 16, 19, 43]. The rate of influx of extracellular calcium in astrocytes mediated by the ionotropic ATP receptor P2X is defined as follows:

$$v_{ATP(P2X)} = k_{ATP(P2X)} G\left([ATP]_{ex}\right) \tag{3}$$

where $G\left([ATP]_{ex}\right) = [ATP]_{ex}^{1.4} / \left(H_{ATP(P2X)} + [ATP]_{ex}^{1.4}\right)$; $[ATP]_{ex}$ is the external concentration of ATP (μM); $H_{ATP(P2X)}$ and $k_{ATP(P2X)}$ are defined in Table 1. The G($[ATP]_{ex}$) function was obtained by fitting the experimental data reported in Nobile et al. [10] which describe the amplitude of the sustained calcium response of the astrocyte against the extracellular ATP concentration. The ATP-evoked calcium response mediated by the activation of a metabotropic ATP receptor coupled to a G-protein, leading to the production of IP_3, is described as follows. The activation of the metabotropic P2Y receptor is described by a very simple biochemical reaction scheme: $ATP + R_{MB} \leftrightarrow ATP - R_{MB}$, where ATP binds to the receptor R_{MB} with forward and reverse rate constants, K_F and K_R, respectively. Let R_0 be the concentration of the metabotropic ATP receptors and $x_F = [ATP - R_{MB}]/R_0$ be the fraction of receptors bound, and then the time evolution of x_F is described by:

$$dx_F/dt = K_F [ATP]_{ex} - x_F \left\{K_R + K_F [ATP]_{ex}\right\} \tag{4}$$

where $[ATP]_{ex}$ is the external concentration of ATP (μM). The solution of this equation satisfying the initial condition $x_F(0) = 0$ is given by $x_F(t) = [ATP]_{ex}/\left(K_D + [ATP]_{ex}\right)$ $[1 - \exp(-t/\tau)]$ where $K_D = K_R/K_F$ is the dissociation constant (see Table 1) and $\tau = 1/\left(K_R + K_F\,[ATP]_{ex}\right)$. By assuming a fast binding kinetics, the reaction $ATP + R_{MB} \leftrightarrow ATP - R_{MB}$ can be assumed to be in equilibrium and therefore it is:

$$x_F(t) = [ATP]_{ex}/\left(K_D + [ATP]_{ex}\right). \tag{5}$$

Therefore, for simplicity, the rate of IP_3 production promoted through this pathway (G-protein and PLCβ activation) is assumed to be determined by

$$\nu_{PLC\beta} = k_{ATP(P2Y)} x_F \tag{6}$$

and the value of the constant $k_{ATP(P2Y)}$ is reported in Table 1.

The explicit formulation of the remaining rate terms appearing in Eqs. 1a–1d are:

$$\nu_{LM} = k_0 \tag{7}$$

$$\nu_{OUT} = k_5 Ca_i \tag{8}$$

$$\nu_{ER(Rel)} = \left\{k_1 + k_2 R Ca_i^2 I^2/\left[\left(K_a^2 + Ca_i^2\right)\left(K_{IP3}^2 + I^2\right)\right]\right\}(Ca_{ER} - Ca_i) \tag{9}$$

$$\nu_{SERCA} = k_3 Ca_i \tag{10}$$

$$\nu_{IP3(Deg)} = k_9 I \tag{11}$$

$$\nu_{PLC\delta} = \nu_7 Ca_i^2/\left(K_{Ca}^2 + Ca_i^2\right) \tag{12}$$

$$\nu_{IP3R(Rec)} - \nu_{IP3R(Inact)} = k_6\left[K_i^2/\left(K_i^2 + Ca_i^2\right) - R\right]. \tag{13}$$

The meanings and the values of the constants are reported in Table 1. In Di Garbo et al. [36], it was shown that the above model is capable of describing, both qualitatively and quantitatively, the experimental results reported in [10]. In particular, it was shown that the model is able to reproduce the ATP-evoked biphasic calcium response (the transient and the sustained phase) in the astrocyte: the transient phase corresponds to the release of calcium from the ER store, while the sustained part is mainly determined by the influx of extracellular calcium mediated by the P2X purinoreceptors. Additional details on this specific topic can be found in Di Garbo et al. [36].

2.4 Neuron–astrocyte–interneuron coupling model

As discussed previously, the experimental results imply that the release of glutamate and ATP by the astrocyte impacts the neural dynamics by modulating the firing activity of neurons and interenurons [12, 14]. Glutamate determines a depolarization of the pyramidal cells, while ATP leads to an increase of inhibition by promoting spike generation in the

interneurons [8, 18, 44–46]. Thus, a minimal neural network model with realistic features must contain astrocytes, excitatory neurons, and inhibitory interneurons. In fact, interneurons receive excitatory inputs from pyramidal cells and then provide feedback inhibition to them by modulating their firing activities [47]. This mechanism is at the core of the existence of an excitatory–inhibitory feedback loop between pyramidal cells and interneurons [47–50]. Then, from these considerations, it follows that the understanding of the mechanisms regulating the neural modulation arising from the astrocytes requires the study of a network of coupled neurons, interneurons, and astrocytes. For obvious complexity reasons, in this paper, only a minimal network consisting of an astrocyte, an excitatory neuron, and an interneuron will be considered. In what follows, it will be assumed that the glutamate released by the astrocyte depolarizes both the pyramidal neuron and the interneuron. An experimental justification for this assumption can be found in Bowser and Khakh [45]. The mechanisms regulating the ATP release from the astrocytes are not well known; thus, for simplicity, it will be assumed here that there is a fixed concentration of extracellular ATP that will be considered as a control parameter. The depolarization of the neuron and the interneuron arising from the release of glutamate from the astrocyte is described by using the model of Nadkarni and Jung [51, 52], which is based on the experimental data of Parpura and Haydon [8]. As discussed previously, the elevation of the intracellular calcium level in astrocytes triggers the release of glutamate from these cells leading to a modulation of the neural activity [4, 5, 8, 11, 12, 20, 42]. Then, the pyramidal cell model, with a soma compartment assuming a diameter of 25 μm, is injected with the following current:

$$I_{\text{astro}} = A_{\text{astro}} H[ln\,(y)] \ln\,(y)\,, \quad y = \left[Ca^{2+}\right]_i - 196.69 \tag{14}$$

where $H(x)$ is the Heaviside function; $A_{\text{astro}} = 2.11\ \mu A/cm^2$; $[Ca^{2+}]_i$ is the cytosolic calcium concentration in the astrocyte in nanomolar units [51, 52]. Concerning the interneuron, the corresponding depolarization current is of the same form as Eq. 14 but with a different value of the constant A_{astro}. In fact, assuming an interneuron diameter of about 15 μm, it follows that $\overline{A}_{\text{astro}} = 6\ \mu A/cm^2$. To get this result, it was implicitly assumed, for simplicity, that the concentration of glutamate close to the pyramidal neuron and the interneuron is of the same order and that the number of glutamate receptors that are activated on each cell is equal. When such assumption does not hold, the value of $\overline{A}_{\text{astro}}$ will be different from the above value. However, by supplemental simulations, it was found that slight changes of the values of these constants do not lead to qualitative changes of the results that will be presented here.

The experimental results found by Bowser and Khakh [45] have shown that the presence of ATP promotes the generation of action potentials in interneurons. It is important to stress again that the current experimental findings suggest that the presence of the ATP does not depolarize the pyramidal neurons [44–46]. In the experimental work of Bowser and Khakh [45], the modulation phenomena of the neural activity arising from ATP were studied on a pair of coupled interneurons and a pair consisting of an interneuron coupled to a pyramidal cell. The results were the following: in the case of a pair of interneurons, the presence of the ATP promoted the generation of action potentials in the presynaptic interneuron leading to an increase of the inhibitory effects on the postsynaptic cell [45]. For the other pair, no depolarization effects were detected on the pyramidal cell, while the increase of the firing probability of the interneuron promoted a hyperpolarization of the pyramidal neuron [45]. To account for these experimental results, the depolarization current on the interneuron is modeled, for simplicity, by

$$I_{\text{ATP}} = A_{\text{ATP}}\,[\text{ATP}]_{\text{ex}} \tag{15}$$

where $[ATP]_{ex}$ is the extracellular concentration of ATP and A_{ATP} is the corresponding amplitude. The value of A_{ATP} was chosen by using the experimental results described in [45]. In fact, it was shown that when the external concentration of the ATP is 100 μM the peak of the depolarizing current evoked on the interneuron was about 36 pA. By inserting these data in Eq. 15, it follows that $A_{ATP} = 0.05\ (\mu A/cm^2)\ (\mu M)^{-1}$.

The pyramidal neuron and the interneuron were described by using the model of Olufsen et al. [53]. In particular, the pyramidal neuron model receiving the depolarizing current I_{astro} due to the release of glutamate from the astrocyte, and an inhibitory synaptic current from the interneuron, is described by the following set of equations:

$$\begin{aligned}
\frac{dV_P}{dt} &= I_p - I_{Na,P} - I_{K,P} - I_M - I_{L,P} - g_i s_i (V_P - V_i) + I_{astro} \\
\frac{dm_P}{dt} &= \alpha_{m,P}(1 - m_P) - \beta_{m,P} m_P \\
\frac{dh_P}{dt} &= \alpha_{h,P}(1 - h_P) - \beta_{h,P} h_P \\
\frac{dn_P}{dt} &= \alpha_{n,P}(1 - n_P) - \beta_{n,P} n_P \\
\frac{dw}{dt} &= (w_\infty - w)/\tau_w,
\end{aligned} \tag{16}$$

where I_p is the stimulation current. Similarly, the interneuron model receiving the depolarizing current $\bar{I}_{astro}$, the excitatory synaptic current from the pyramidal neuron, and the depolarizing current I_{ATP} are described by the following equations:

$$\begin{aligned}
\frac{dV_{IN}}{dt} &= I_{IN} - I_{Na,IN} - I_{K,IN} - I_{L,IN} - g_e s_e (V_{IN} - V_e) + \bar{I}_{astro} + I_{ATP} \\
\frac{dm_{IN}}{dt} &= \alpha_{m,IN}(1 - m_{IN}) - \beta_{m,IN} m_{IN} \\
\frac{dh_{IN}}{dt} &= \alpha_{h,IN}(1 - h_{IN}) - \beta_{h,IN} h_{IN} \\
\frac{dn_{IN}}{dt} &= \alpha_{n,IN}(1 - n_{IN}) - \beta_{n,IN} n_{IN},
\end{aligned} \tag{17}$$

where I_{IN} is the stimulation current. In the previous equations, V_p and V_{IN} are the membrane potentials of the pyramidal cell and of the interneuron, respectively. The constant g_i (g_e) represents the value of the inhibitory (excitatory) conductance: the adopted values are those reported in Olufsen et al. [53] and they are $g_i = 1\ mS/cm^2$, $g_e = 0.3\ 1\ mS/cm^2$. The value of the reversal potential of the excitatory synapse is $V_e = 0$ mV, while that of the inhibitory synapses is $V_i = -80$ mV. For both the neuron and the interneuron model, $I_{Na,P}$ and $I_{Na,IN}$ are the sodium currents; $I_{K,P}$ and $I_{K,IN}$ are the potassium currents; $I_{L,P}$ and $I_{L,IN}$ are the passive currents (leakage). Lastly, I_M is a typical ionic current of pyramidal cells contributing to slow spike frequency adaptation. The explicit expression of all these currents is the following: $I_{Na,P,IN} = g_{Na} m_{P,IN}^3 h_{P,IN}(V_{P,IN} - V_{Na})$, $I_{K,P,IN} = g_K n_{P,IN}^4 (V_{P,IN} - V_K)$, $I_{L,P,IN} = g_L (V_{P,IN} - V_L)$, $I_M = g_M w (V_P - V_M)$. The corresponding

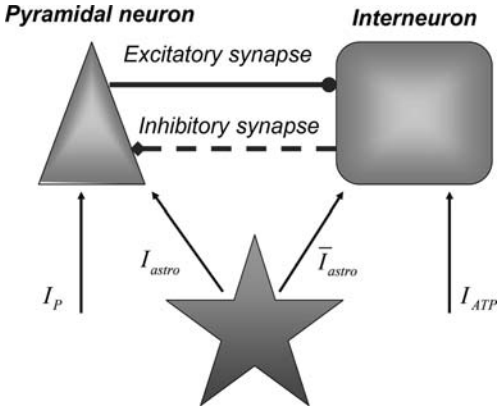

Fig. 1 A schematic diagram showing the minimal neural network model studied in this paper

activation and inactivation variables are defined as follows: $\alpha_{m,\mathrm{P,IN}} = [0.032(V_{\mathrm{P,IN}}+54)]/[1-\exp(-(V_{\mathrm{P,IN}}+54)/4)]$, $\beta_{m,\mathrm{P,IN}} = [0.28(V_{\mathrm{P,IN}}+27)]/[\exp((V_{\mathrm{P,IN}}+27)/5)-1]$, $\alpha_{h,\mathrm{P,IN}} = [0.128\exp(-(V_{\mathrm{P,IN}}+50))]/18$, $\beta_{h,\mathrm{P,IN}} = 4/[1+\exp(-(V_{\mathrm{P,IN}}+27)/5)]$, $\alpha_{n,\mathrm{P,IN}} = [0.032(V_{\mathrm{P,IN}}+52)]/[1-\exp(-(V_{\mathrm{P,IN}}+52)/5)]$, $\beta_{n,\mathrm{P,IN}} = 0.5\exp(-(V_{\mathrm{P,IN}}+57)/40)$, $w_\infty = 1/1+\exp(-(V_{\mathrm{P}}+35)/10)$, and $\tau_w = 400/[3.3\exp((V_{\mathrm{P}}+35)/20)+\exp((V_{\mathrm{P}}+35)/20)]$. The functions $s_{\mathrm{i}}(t)$ and $s_{\mathrm{e}}(t)$ describe the time evolution of the inhibitory and excitatory currents, respectively. The equations defining their time evolution are given by:

$$\frac{\mathrm{d}s_{\mathrm{e}}}{\mathrm{d}t} = T_{\mathrm{e}}(V_{\mathrm{P}})(1-s_{\mathrm{e}}) - s_{\mathrm{e}}/\tau_{\mathrm{e}} \tag{18a}$$

$$\frac{\mathrm{d}s_{\mathrm{i}}}{\mathrm{d}t} = T_{\mathrm{i}}(V_{\mathrm{IN}})(1-s_{\mathrm{i}}) - s_{\mathrm{i}}/\tau_{\mathrm{i}} \tag{18b}$$

where $T_{\mathrm{e}}(V_{\mathrm{P}}) = 5[1+\tanh(V_{\mathrm{P}}/4)](\mathrm{ms}^{-1})$ and $T_{\mathrm{i}}(V_{\mathrm{IN}}) = 2[1+\tanh(V_{\mathrm{IN}}/4)](\mathrm{ms}^{-1})$ with $\tau_{\mathrm{e}} = 2$ ms and $\tau_{\mathrm{i}} = 10$ ms. In Fig. 1, a schematic representation of this minimal neural network constituted by the astrocyte, the neuron, and the interneuron is shown.

To describe the production of IP_3 in the astrocyte triggered by the discharge of the excitatory cell, the simple mathematical model used by Nadkarni and Jung [51, 52] is adopted here. Let r_{PY} be the rate of production of IP_3 when an action potential is generated by the pyramidal cell and $V_{\mathrm{Th}} = -50$ mV be a membrane potential threshold value. Then, it is assumed that there is a production of IP_3 in the astrocyte only when $V_{\mathrm{p}} > V_{\mathrm{Th}}$ and the corresponding rate, to be added to the right-hand side of Eq. 1d, is defined by $\nu_{\mathrm{PY}} = r_{\mathrm{PY}} H(V_{\mathrm{p}} - V_{\mathrm{Th}})$, where $H(x)$ is the Heaviside function.

3 Results

3.1 Dynamical properties of the new model describing calcium dynamics in the astrocyte

Let us consider the model describing calcium dynamics in the astrocyte defined in Section 2.3. Let us consider the case in which the astrocyte is isolated and in the presence of a given concentration of extracellular ATP. First of all, we are interested to search for the

corresponding stationary states, and this is equivalent to finding all solutions of the following system of equations:

$$\begin{aligned} \nu_{\mathrm{LM}} + \nu_{\mathrm{CCE}} + \nu_{\mathrm{ATP(Ionotropic)}} - \nu_{\mathrm{OUT}} + \nu_{\mathrm{ER(Rel)}} - \nu_{\mathrm{SERCA}} &= 0 \\ \nu_{\mathrm{SERCA}} - \nu_{\mathrm{ER(Rel)}} &= 0 \\ \nu_{\mathrm{IP3R(Rec)}} - \nu_{\mathrm{IP3R(Inact)}} &= 0 \\ \nu_{\mathrm{PLC}} + \nu_{\mathrm{PLC}} - \nu_{\mathrm{IP3(Deg)}} &= 0. \end{aligned} \tag{19}$$

By using the explicit expression of the rates, it can be shown that the search for the corresponding solutions is equivalent to finding the roots of the following nonlinear equation:

$$k_0 + \frac{k_{\mathrm{CCE}} H_{\mathrm{CCE}}^2}{H_{\mathrm{CCE}}^2 + g(\mathrm{Ca}_i)} + \frac{k_{\mathrm{ATP(P2X)}[\mathrm{ATP}]_{\mathrm{E}}^{1.4}}}{H_{\mathrm{ATP(P2X)}} + [\mathrm{ATP}]_{\mathrm{E}}^{1.4}} - k_5 \mathrm{CA}_i = 0 \tag{20}$$

where the function $g(\mathrm{Ca}_i) = \mathrm{Ca}_{\mathrm{ER}}$ is defined by

$$\mathrm{Ca}_{\mathrm{ER}} = g\left(\mathrm{Ca}_i\right) = \mathrm{Ca}_i + \frac{k_3 \mathrm{Ca}_i}{\left\{k_1 + \frac{k_2 R \mathrm{Ca}_i^2 I^2}{\left(k_a^2 + \mathrm{Ca}_i^2\right)\left(k_{\mathrm{IP3}}^2 + I^2\right)}\right\}}. \tag{21}$$

The remaining variables characterizing the stationary state is given by:

$$\begin{aligned} R &= \frac{k_i^2}{k_i^2 + \mathrm{Ca}_i^2} \\ I &= k_9^{-1} \left\{ \frac{K_{\mathrm{ATP(P2Y)}} [\mathrm{ATP}]_{\mathrm{E}}}{k_{\mathrm{D}} + [\mathrm{ATP}]_{\mathrm{E}}} + \frac{\nu_7 \mathrm{Ca}_i}{k_{\mathrm{Ca}}^2 + \mathrm{Ca}_i^2} \right\}. \end{aligned} \tag{22}$$

In the stationary state, the calcium fluxes through the cellular membrane satisfy the equation $\nu_{\mathrm{LM}} + \nu_{\mathrm{CCE}} + \nu_{\mathrm{ATP(Ionotropic)}} = \nu_{\mathrm{OUT}} = k_5 \mathrm{Ca}_i$. Such a constraint implies that in this condition the quantity of calcium entering the cell is completely balanced by that extruded from the astrocyte. The importance of the membrane transport of Ca^{2+} in the control of calcium oscillations was shown recently by Sneyd et al. [54]. Similar results were obtained also by Lavrentovich and Hemkin [55]. Moreover, it was shown experimentally that an increase of the intracellular calcium concentration in the astrocyte promotes the generation of oscillations [56]. Therefore, we start by investigating how the values of the parameter k_5 affect the stability properties of the stationary states of the adopted calcium model. To this aim, the stability of each stationary state of Eqs. 1a–1d was assessed by determining the signs of the eigenvalues of the corresponding Jacobian matrix. In Fig. 2a, the corresponding results in the case in which $[\mathrm{ATP}]_{\mathrm{ex}} = 0$ are reported. These data show that there is a critical interval of k_5 values where the corresponding stationary state is unstable and calcium oscillations occur. It can be shown that the changes of stability of the stationary state, leading to the generation of periodic solutions, occur through a Hopf bifurcation. These data also show that, apart from a small interval of k_5 values, the increase of the rate of extrusion of the intracellular calcium from the astrocyte determines a progressive reduction of the oscillation amplitude. This last fact is in agreement with the experimental results reported in Parri and Crunelli [56] and also with those of Lavrentovich and Hemkin [55] and Sneyd et al. [54]. On the contrary, there is an increase of the period of calcium oscillation as the parameter k_5 increases.

An important difference of the model used in this paper with that employed by Lavrentovich and Hemkin [55] and Sneyd et al. [54] concerns the modulation effects arising from the presence of the extracellular ATP. Thus, a relevant problem—worthy to be investigated—is to understand how the above results change when extracellular ATP is present. The corresponding results are reported in Fig. 2b and clearly show that the presence of small concentration of extracellular ATP ($[ATP]_{ex} = 0.05\ \mu M$) strongly impacts the astrocytic capability to generate calcium oscillations. In fact, now there is a drastic

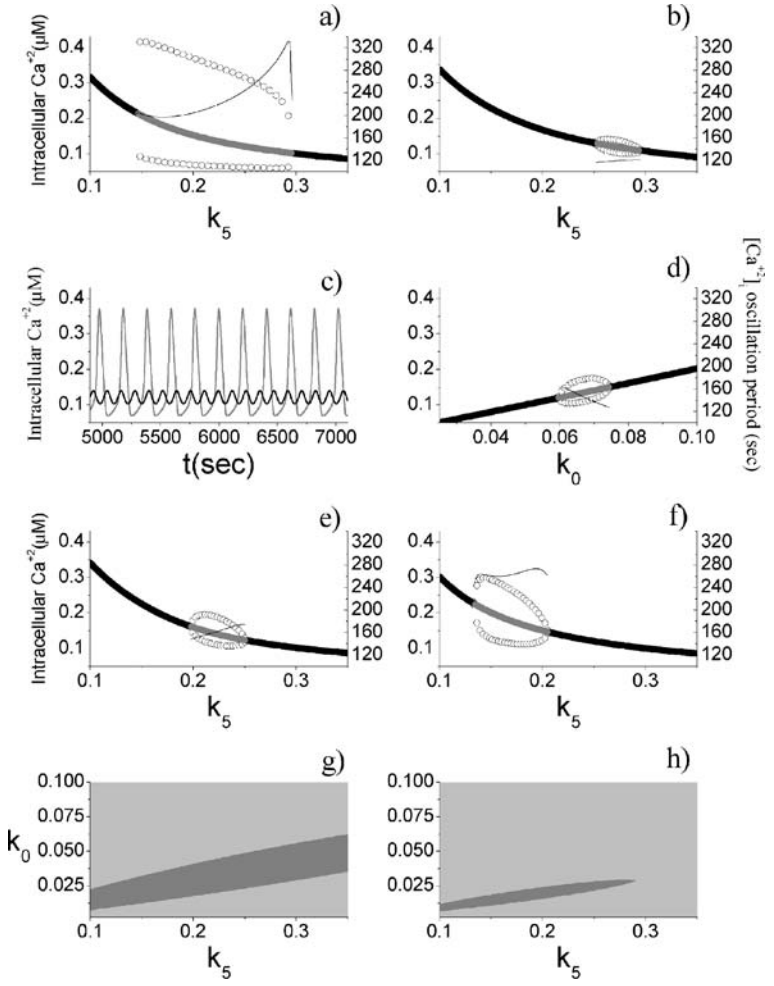

Fig. 2 Dynamical properties of the astrocytic calcium model. **a** $[ATP]_{ex} = 0\ \mu M$, with the oscillation period shown on the right axis. **b** Same as **a**, but with $[ATP]_{ex} = 0.05\ \mu M$. **c** The *gray line* corresponds to $[ATP]_{ex} = 0\ \mu M$, $k_5 = 0.2\ s^{-1}$, the *black line* to $[ATP]_{ex} = 0\ \mu M$, $k_5 = 0.2\ s^{-1}$. **d** $[ATP]_{ex} = 0\ \mu M$. **e** $[ATP]_{ex} = 0\ \mu M$, $k_3 = 0.25\ s^{-1}$. **f** $[ATP]_{ex} = 0\ \mu M$, $k_2 = 0.05\ s^{-1}$. **g** Two-dimensional parameter plot of the states of the calcium model for $[ATP]_{ex} = 0\ \mu M$. The *light gray region* corresponds to stable stationary states, while the *gray* one to oscillatory regimes. **h** Same as **g**, but with $[ATP]_{ex} = 0.05\ \mu M$. For **a**, **b**, **d**, **e**, and **f**, the *thick black lines* represent stable stationary states, while the *gray* ones the unstable states. The *open circles* represent the oscillation amplitudes

reduction of both the interval of k_5 values where oscillations occur and of the corresponding amplitudes. The data also show those in this case the variations of the oscillation period are smaller than that occurring in the absence of ATP. In Fig. 2c, some examples of calcium oscillations in the two situations are reported. In conclusion, these data suggest that there is a range of values of the parameter k_5 in which the calcium oscillations can be used to encode frequency information for $[ATP]_{ex} = 0$.

Next, by keeping k_5 fixed at the value given in Table 1, the dynamical behavior of the intracellular calcium was studied as a function of the rate of leakage influx of calcium from the extracellular medium (k_0). The corresponding data, obtained in absence of ATP, are reported in Fig. 2d. The comparison of these results with those reported in panel Fig. 2a indicates that the amplitude of the oscillations is smaller and that the period exhibits a reduced variability. Moreover, in agreement with the experimental results of Parri and Crunelli [56], the increase of the intracellular calcium level determines a decrease of the period of the calcium oscillations. Effects similar to those already discussed occur when ATP is present (data not shown).

Which are the effects of inhibiting the SERCA pump on the astrocytic calcium oscillations? Experimentally, it was shown that the inhibition of this pump by cyclopiazonic acid or by thapsigargin produces a decrease of the amplitude and of the frequency of the calcium oscillations in the astrocyte [56–58]. To test whether the model is able to reproduce such results, the simulations were carried out by halving the parameter values describing the rate of the SERCA pump (the adopted value was $k_3 = 0.25\ s^{-1}$). The comparison of the corresponding results reported in Fig. 2e with those of Fig. 2a shows that the inhibition of the SERCA pump leads to: (1) a reduction of the interval of k_5 values where oscillations can occur, (2) a decrease of the amplitudes of calcium oscillations, and (3) a decrease of the period of oscillations. The result 2 is in agreement with the experimental results, while 3 is at odds. A similar result was also found by Lavrentovich and Hemkin [55]. The explanation of why 3 is at odds with the experimental result is not at our disposal and a deeper investigation will be carried out elsewhere.

Experimentally, it was shown that a reduction of the influx of calcium from the endoplasmic reticulum to the cytoplasm (mediated by the IP_3 receptors) does not promote the emergence of calcium oscillations [56, 59]. Therefore, to mimic the experimental conditions, the simulations of the calcium model were performed by adopting a smaller value of the parameter k_2 describing the amplitude of such flux. The corresponding results are reported in Fig. 2f and they are qualitatively in agreement with the experimental findings.

In Fig. 2g, a two-dimensional parametric plot characterizing the system's dynamical regimes when both k_0 and k_5 vary is reported. It can be seen that there is a parameter space region where oscillations can occur. Moreover, the maintenance of the oscillation regime for increasing k_5 values requires also higher k_0 values. When extracellular ATP is present, there is a drastic reduction of the area of the parameter space where oscillations can occur (Fig. 2h).

In conclusion, the above results clearly show that calcium transport across the membrane plays an important role in the genesis of astrocytic calcium oscillations.

3.2 Pyramidal neuron and astrocyte

Let us study how the release of neurotransmitter from the astrocyte impacts the firing activity of the pyramidal neuron in the absence of inhibition arising from the interneuron.

To this aim, the pyramidal neuron model was stimulated with a depolarizing current I_p for 10 s alone. Then, the corresponding firing triggers the production of IP_3 which causes an elevation of the internal calcium level in the astrocyte. When the $[Ca^{+2}]_i$ goes above the threshold, a release of glutamate from the astrocyte occurs, and this causes an additional depolarization of the pyramidal neuron (see Eq. 14). The simulation results are shown in Fig. 3 for different r_{PY} values. From the top panels, it can be seen that when the level of the internal calcium level goes above the threshold a depolarization current is generated in the pyramidal cell. This event provokes the firing of the neuron in the region where

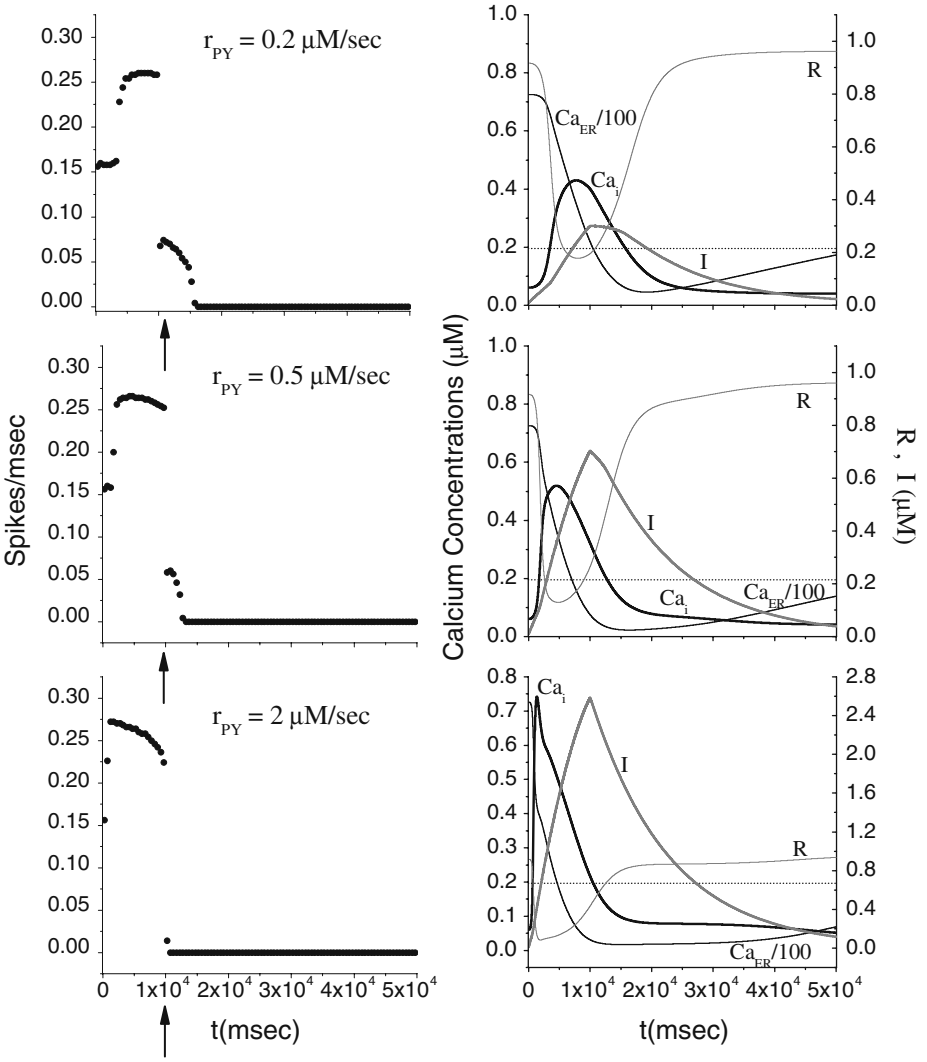

Fig. 3 Effects on the pyramidal neuron dynamics induced by change of rate of production of IP_3. For all *panels*, $[ATP]_{ex} = 0$ μM. The bin size to estimate the average firing rate was 500 ms. The *dotted line* represents the calcium threshold

the stimulation is absent. However, the duration of this additional firing is about 5 s and is strongly dependent on the internal calcium level in the astrocyte: when these values get smaller than the threshold, the firing stops. The simulations shown in the middle and bottom panels indicate that the increase of the parameter r_{PY} determines a reduction of the time interval where the generation of action potentials occurs in the absence of the stimulation current. The right panels of Fig. 3 show that the increase of r_{PY} leads to a faster elevation and decay of the internal calcium concentration in the astrocyte. Thus, the duration of the time interval in which the firing occurs in the absence of stimulation decreases toward zero. In conclusion, these results suggest that for the chosen parameter values the indefinite firing of the pyramidal neuron in the absence of stimulation cannot occur. These results are in disagreement with those of Nadkarni and Jung [51, 52] that instead predict an indefinite firing of the pyramidal neuron for suitable r_{PY} values. These contrasting results can be accounted for by the different calcium membrane fluxes between the two models. In fact, additional simulations performed with our model have shown that a reduction of the value of the constant k_5 (for instance, $k_5 = 0.15\ s^{-1}$) describing the calcium extrusion rate from the cell leads to indefinite firing as predicted by Nadkarni and Jung [51, 52] (data not shown). It is worth mentioning that in the calcium model adopted by Nadkarni and Jung [51, 52, 61] the Ca^{+2} fluxes through the cellular membrane are absent.

How do these results change when, while keeping the r_{PY} value fixed, the stimulation current is increased? The result of the simulations (data not shown) indicates that the increase of the amplitude of the stimulation current leads to a reduction of the time interval in which the firing of the neuron occurs without stimulation. This behavior can be ascribed to the fact that a larger firing frequency of the neuron leads to a faster increase and decrease of the calcium level in the astrocyte.

Let us consider now the effect of ATP on the dynamical behavior of the neuron. The corresponding simulation results for different concentrations of ATP are shown in Fig. 4. The presence of ATP leads to the activation of purinergic receptors (ionotropic and metabotropic) that promote the enhancement of the calcium response of the astrocyte. For $[ATP]_{ex} = 1.5\ \mu M$, the stationary calcium level of the cell reaches a value greater than that obtained in the right panels of Fig. 3 but nonetheless remains below the threshold. When the ATP level is further increased (middle panels), the steady-state calcium level goes above the threshold, leading to the generation of firing in the neuron in the absence of stimulation, although with a lower firing rate. Taken together, the previous results suggest that the presence of ATP strongly impacts the dynamical behavior of the neuroglial network. How do these results change when the desensitization effect of ATP receptors are included in the model? In fact, the data reported in Nobile et al. [10] clearly show that the P2X receptor desensitizes when exposed for several seconds to ATP. Thus, a very simple model describing the desensitization process of the ionotropic purinergic receptor was introduced in the calcium model. In particular, it was assumed that the rate $\nu_{ATP(P2X)}$ (see Eq. 3) is now defined as $\nu_{ATP(P2X)} = k_{ATP(P2X)} G\left([ATP]_{ex}\right) D(t)$, where $D(t) = C_N\left(1 - e^{-(t-t*)/\tau_{off}}\right)e^{-(t-t*)/\tau_{off}}$ is a solution of the equation $\ddot{D}(t) + P\dot{D}(t) + QD(t) = 0$ with $P = (2/\tau_{off} + 1/\tau_{on})$ and $Q = (1/\tau_{off} + 1/\tau_{on})/\tau_{off}$; moreover, $\tau_{on} = (2\ \mu M s)/[ATP]_{ex}$, $\tau_{off} = 400$ s and C_N is a normalization constant such that $D(t) \leq 1$. The constants τ_{off} and τ_{on} were chosen in order to reproduce qualitatively and quantitatively the experimental data reported in Nobile et al. [10]. The corresponding simulation results describing the desensitization effects of the ionotropic purinergic receptor are shown in the bottom panels of Fig. 4. The comparison of these data with those illustrated in the middle panels shows that

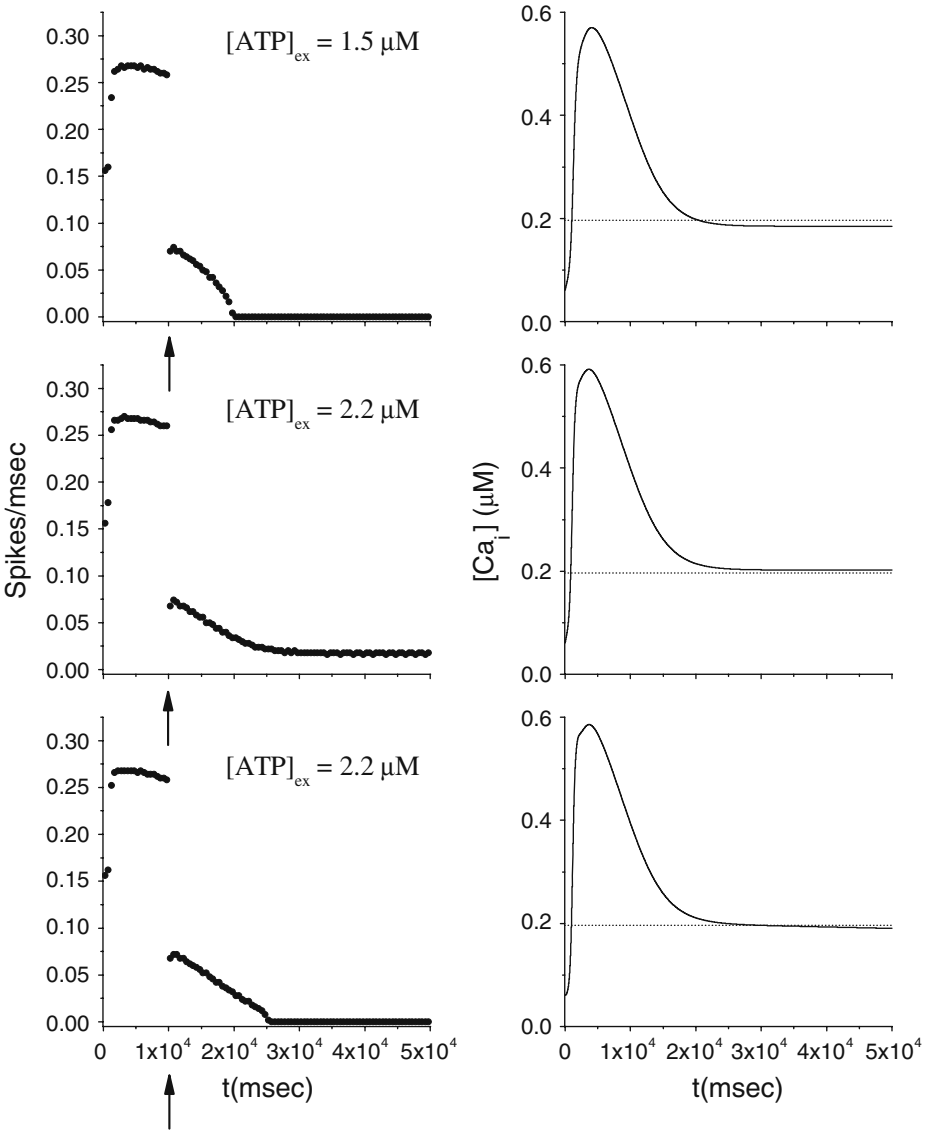

Fig. 4 Effects on the pyramidal neuron dynamics determined by the ATP concentration. For all *panels*, $r_{PY} = 0.2$ μM/s. In the *bottom panels*, results in the presence of desensitization of the P2X receptor are shown. The bin size to estimate the average firing rate was 500 ms. The *dotted line* represents the calcium threshold

the presence of the desensitization of the P2X receptor stops the firing activity of the neuron for t values greater than about 25 s. The comparison of these results with those shown in the bottom panels shows that this occurs because the desensitization process causes a gradual decrease of the calcium level in the astrocyte until it falls below the threshold.

3.3 Pyramidal neuron, interneuron, and astrocyte

Let us consider now a more realistic situation of a network consisting of the pyramidal neuron, the interneuron, and the astrocyte. To simplify the discussion, it is assumed that desensitization of the P2X receptor does not occur. As discussed in Section 2.4, the pyramidal neuron excites the interneuron through an excitatory synapse, while the interneuron feedback inhibits it by an inhibitory synapse. Moreover, if the calcium level of the astrocyte goes above the threshold, then both the neuron and the interneuron will receive excitatory currents (see Section 2.4). Lastly, the presence of ATP leads to the generation of an excitatory current in the interneuron alone. To have a more realistic network, it is assumed that the pyramidal neuron is injected with a depolarizing current I_p mimicking some sensory input, while for the interneuron we have $I_{IN} = 0$. The results of the simulations of this network are reported in Fig. 5 for the case $r_{PY} = 0.2$ μM/s. When $[ATP]_{ex} = 0$, the firing of the pyramidal neuron leads to an increase of the calcium level of the astrocyte above the threshold. When this occurs, the two additional depolarizing currents (arising from the release of glutamate from the astrocyte) cause a very fast increase of the firing rate of the interneuron that then stops the firing of the pyramidal neuron in the region where $I_p = 0$. When the calcium level of the astrocyte falls below the threshold, then the firing rate of the interneuron also ceases. The simulation data obtained when an ATP concentration of 2.2 μM is present are shown in Fig. 5c, d. In this case, the stationary value of the calcium concentration is greater than the threshold and therefore the firing of the interneuron never stops. For $t > 10$ s, the depolarization level of the pyramidal neuron is not sufficient to overcome the inhibitory barrage coming from the interneuron and consequently its firing ceases. The data reported in Fig. 5e, f show clearly that the inhibitory effects play a key role in the determination of the dynamical behavior of the network. They were obtained by decreasing the value of g_i and comparison with Fig. 5c, d shows that now the firing of the pyramidal cell never stops, although with a lower firing rate. A dramatic change of the previous results occurs when the parameter value describing the amplitude of the extrusion rate of calcium from the cytoplasm (k_5) is slightly increased. Now, even in the presence of ATP, the firing activities of both cells stop for $t > 10$ s (Fig. 5g, h).

To get a more general picture of the network dynamics, bifurcation diagrams were computed. The results of the corresponding simulations are reported in Fig. 6 and show how the maximum and minimum value of V_p (or of V_{IN}) vary as the control parameter is varied. The simulations were carried out by numerical integration of the 15 coupled differential equations up to 100 s for each value of the control parameter. Then, the quantities reported in the graphs were estimated after discarding a transient time amounting to the first 90 s. The data reported in Fig. 6a show the dependence of the neural activities on the parameter r_{PY}, which describes the rate of production of IP_3 triggered by the firing of the pyramidal cell. The corresponding results show that the increase of the parameter r_{PY} never leads to the indefinite firing of both cells. The results shown in Fig. 6b indicate that the change of the amplitude of the stimulation current I_p does not lead to the indefinite firing of both cells either. A drastic change occurs when the extracellular ATP is present and in Fig. 6c the corresponding results when its concentration is varied are shown. It can be seen that there is a critical value of $[ATP]_{ex}$ (2.1 μM) above which the interneuron fires indefinitely. Then, the presence of the inhibition exerted by the interneuron impedes the firing of the pyramidal neuron. It can be seen from the data reported on the right axis that the oscillation period of the interneuron is a decreasing function of ATP. This can be explained by the fact that the calcium level in the astrocyte increases as the extracellular concentration of

ATP increases. For $[ATP]_{ex} < 2.1$ μM, both neural models cannot fire indefinitely in the absence of stimulation. In Fig. 6d, the data obtained by varying the parameter k_5 and with $[ATP]_{ex} = 2.2$ μM are reported. It can be seen that there is a critical value k_5^* such that for

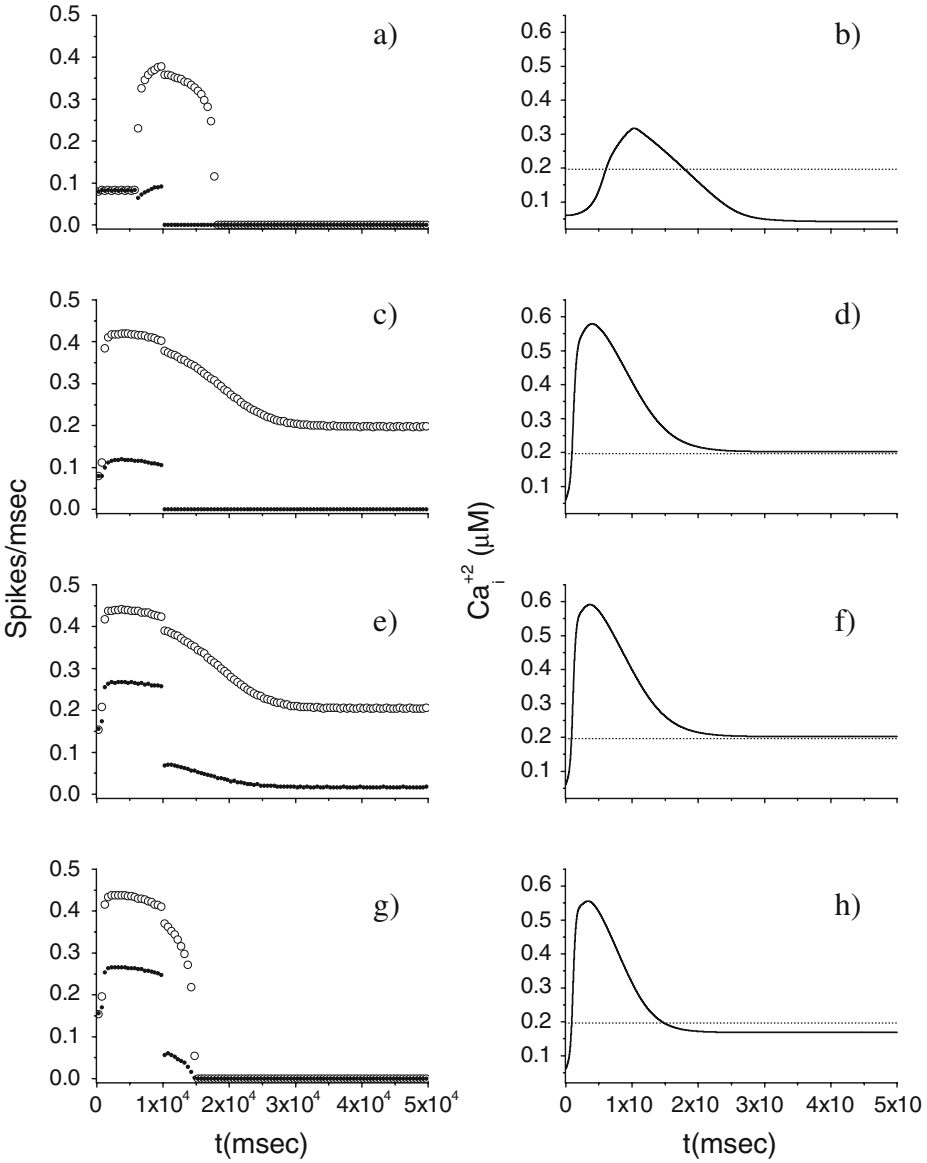

Fig. 5 Dynamical properties of the network of neuron, interneuron, and astrocyte. **a** and **b** $[ATP]_{ex} = 0$ μM, $g_e = 0$ mS/cm^2, $g_i = 1$ mS/cm^2. **c** and **d** $[ATP]_{ex} = 2.2$ μM, $g_e = 0.3$ mS/cm^2, $g_i = 1$ mS/cm^2. **e** and **f** $[ATP]_{ex} = 2.2$ μM, $g_e = 0.3$ mS/cm^2, $g_i = 0.01$ mS/cm^2. **g** and **h** $[ATP]_{ex} = 2.2$ μM, $g_e = 0.3$ mS/cm^2, $g_i = 0.01$ mS/cm^2 and $k_5 = 0.6$ s^{-1}. For all *panels*, $r_{PY} = 0.2$ μM/s. The *dotted line* represents the calcium threshold

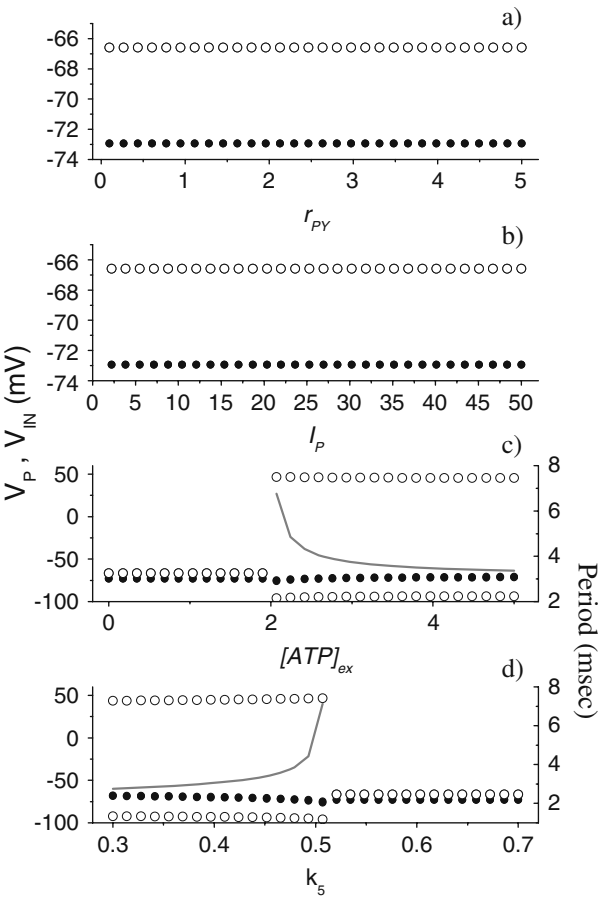

Fig. 6 Bifurcation diagrams showing the dependence of the dynamical behavior of the full neural network when some relevant parameters change. **a** $[ATP]_{ex} = 0$ μM, $I_p = 20$ μA/cm^2, $g_e = 0.3$ mS/cm^2, $g_i = 1$ mS/cm^2, $k_5 = 0.5$ s^{-1}. **b** $[ATP]_{ex} = 0$ μM, $r_{PY} = 0.2$ μM/s, $g_e = 0.3$ mS/cm^2, $g_i = 1$ mS/cm^2, $k_5 = 0.5$ s^{-1}. **c** $I_p = 20$ μA/cm^2, $r_{PY} = 0.2$ μM/s, $g_e = 0.3$ mS/cm^2, $g_i = 1$ mS/cm^2, $k_5 = 0.5$ s^{-1}. **d** $[ATP]_{ex} = 2.2$ μM, $I_p = 20$ μA/cm^2, $r_{PY} = 0.2$ μM/s, $g_e = 0.3$ mS/cm^2, $g_i = 1$ mS/cm^2. For all *panels*, the *black solid circles* correspond to the pyramidal neuron, while the *open circles* to the interneuron. The *gray lines* in **c** and **d** represent the firing period of the interneuron

$k_5 > k_5^*$ both cells stop firing. The data reported on the right-hand axis of 6d show that for $k_5 > k_5^*$ the firing period of the interneuron is an increasing function of this parameter. This behavior arises because the increase of k_5 causes a reduction of the calcium level in the astrocyte and then a smaller depolarizing current in the interneuron.

4 Discussion and conclusions

A minimal biophysical neural network model consisting of a pyramidal neuron, an interneuron, and an astrocyte was introduced. For its complexity, this dynamical system was mainly investigated by means of numerical simulation. It was shown that the dynamical properties of the astrocytic calcium model are sensitive to the fluxes of calcium through the cellular membrane. In the absence of ATP, the calcium model can be used to encode frequency information when the parameter k_5 is varied. It was also found, in agreement with the experimental results, that the increase of the calcium concentration in the astrocyte

determines a decrease of the oscillation period. Moreover, the model is able to reproduce some experimental results. It was also shown that the presence of ATP does not promote the emergence of calcium oscillations. Lastly, the results of the numerical simulation show that the variation of the parameter describing the functioning of the SERCA pump and of the IP_3 receptors on the ER has a strong influence on the calcium dynamics.

The results of the simulations of the pyramidal neuron model, coupled with the astrocyte, show that in the absence of ATP the pyramidal neuron cannot fire indefinitely when the stimulation current is off. The presence of the ATP or the change of the parameter k_5 produces a drastic change in the above results. It was found that also the desensitization process of the P2X receptor has a strong effect on the dynamics of the network. When the interneuron was included in the network, it was found that the pyramidal neuron is strongly modulated by this last cell and its firing always stops. The previous results, interpreted from a biological point of view, suggest that the hypothesis that astrocytes could be implicated in the generation of epileptic phenomena must be considered carefully.

Lastly, let us discuss some possible improvements and generalizations of the model used here. Relative to the biophysical properties of the P2X7 receptor, a possible extension of the calcium model employed in this paper can be achieved by the inclusion of a kinetic model of this receptor (see Egan et al. [60] for additional details). In this case, the calcium entry mediated by the receptor will be time dependent and interesting new dynamical effects—may be expected to occur. Another possible extension of the calcium model is the inclusion of a realistic dynamics of ATP release from the astrocyte. The mechanisms driving this process are not well understood, although there are some direct and indirect evidences suggesting that IP_3 is involved. Then, it should be interesting to investigate the dynamical behavior of the network in the absence of extracellular ATP. Because neuron and astrocytes are spatially extended objects, another generalization of the model could be the inclusion of a spatial network geometry to study the propagation of calcium waves.

There is experimental evidence indicating that the P2X7 receptor exhibits different conduction states defined by their relative permeability to large ions [1, 11, 16, 19, 60]. For instance, the P2X7 receptor could increase the diameter of its conducting pore during sustained application of ATP. Then, it should be interesting to investigate the effect of this phenomenon on the network dynamics.

A limitation of the network model used here is the implicit assumption that some processes, like synaptic transmission or ATP diffusion, occur without time delay. Therefore, a more realistic version of the adopted network model could be the inclusion of suitable delays to study how they affect the dynamical patterns of the neural–glial population.

References

1. Haydon, P.G., Carmignoto, G.: Astrocyte control of synaptic transmission and neurovascular coupling. Physiol. Rev. **86**, 1009–1031 (2006). doi:10.1152/physrev.00049.2005
2. Kandel, E.R., Schwartz, J.H., Jessell, T.M.: Principles of Neural Science. McGraw-Hill, New York (2000)
3. Finkbeiner, S.M.: Glial calcium. Glial **9**, 83–104 (1993). doi:10.1002/glia.440090202
4. Parpura, V., Basarsky, T.A., Liu, F., Jeftinija, K., Jeftinija, S., Haydon, P.G.: Glutamate-mediated astrocyte-neuron signalling. Nature **369**, 744–747 (1994). doi:10.1038/369744a0
5. Porter, J.T., McCarthy, K.D.: Hippocampal astrocytes in situ respond to glutamate released from synaptic terminals. J. Neurosci. **16**, 5073–5081 (1996)
6. Porter, J.T., McCarthy, K.D.: Astrocytic neurotransmitter receptors in situ and in vivo. Prog. Neurobiol. **51**, 439–455 (1997). doi:10.1016/S0301-0082(96)00068-8

7. Kang, J., Jiang, L., Goldman, S.A., Nedergaard, M.: Astrocyte-mediated potentiation of inhibitory synaptic transmission. Nat. Neurosci. **1**, 683–692 (1998). doi:10.1038/3684
8. Parpura, V., Haydon, P.: Physiological astrocytic calcium levels stimulate glutamate release to modulate adjacent neurons. Proc. Natl. Acad. Sci. U. S. A. **97**, 8629–8634 (2000). doi:10.1073/pnas.97.15.8629
9. Wang, Z., Haydon, P.G., Yeung, E.S.: Direct observation of calcium-independent intercellular ATP signalling in astrocytes. Anal. Chem. **72**, 2001–2007 (2000). doi:10.1021/ac9912146
10. Nobile, M., Monaldi, I., Alloiso, S., Cugnoli, C., Ferroni, S.: ATP-induced, sustained signalling in cultured rat cortical astrocytes: evidence for a non-capacitive, P2X7-like-mediated calcium entry. FEBS Lett. **538**, 71–76 (2003). doi:10.1016/S0014-5793(03)00129-7
11. Fellin, T., Carmignoto, G.: Neuron-to-astrocyte signalling in the brain represents a distinct multifunctional unit. J. Physiol. **559.1**, 3–15 (2004)
12. Perea, G., Araque, A.: Synaptic regulation of the astrocyte calcium signal. J. Neural Transm. **112**, 127–135 (2005). doi:10.1007/s00702-004-0170-7
13. Zhang, Q., Haydon, P.G.: Roles for gliotransmission in the nervous system. J. Neural Transm. **112**, 121–125 (2005). doi:10.1007/s00702-004-0119-x
14. Koizumi, S., Fujishita, K., Inoue, K.: Regulation of cell-to-cell communication mediated by astrocytic ATP in the CNS. Purinergic Signal. **1**, 211–217 (2005). doi:10.1007/s11302-005-6321-y
15. Duan, S., Anderson, C.M., Keung, E.C., Chen, Y., Swanson, R.A.: P2X7 receptor-mediate release of excitatory amino acids from astrocytes. J. Neurosci. **23**, 1320–1328 (2003)
16. Fields, R.D., Burnstock, G.: Purinergic signalling in neuron-glia interactions. Nat. Rev., Neurosci. **7**, 423–436 (2006). doi:10.1038/nrn1928
17. Pankratov, Y., Lalo, U., Krishtal, O., Verkhratsky, A.: Ionotropic P2X purinoreceptors mediate synaptic transmission in rat pyramidal neurones of layer II/III of somato-sensory cortex. J. Physiol. **542**(2), 529–536 (2002). doi:10.1113/jphysiol.2002.021956
18. Zhang, J.M., Wang, H.K., Ye, C.Q., Ge, W., Chen, Y., Jiang, Z.L., Wu, C.P., Poo, M.M., Duan, S.: ATP released by astrocytes mediates glutamatergic activity-dependent heterosynaptic suppression. Neuron **40**, 971–982 (2003). doi:10.1016/S0896-6273(03)00717-7
19. Khakh, B.S.: Molecular physiology of P2X receptors and ATP signalling at synapses. Nat. Rev. Neurosci. **2**, 165–174 (2001). doi:10.1038/35058521
20. Pasti, L., Volterra, A., Pozzan, T., Carmignoto, G.: Intracellular calcium oscillations in astrocytes: a highly plastic, bidirectional form of communication between neurons and astrocytes in situ. J. Neurosci. **17**, 7817–7830 (1997)
21. Cornell-Bell, A.H., Finkbeiner, S.M., Cooper, M.S., Smith, S.J.: Glutamate induces calcium waves in cultured astrocytes: long-range glial signalling. Science **247**, 470–473 (1990). doi:10.1126/science.1967852
22. Volterra, A., Meldolesi, J.: Astrocytes, from brain glue to communication elements: the revolution continues. Nat. Rev. Neurosci. **6**, 626–640 (2005). doi:10.1038/nrn1722
23. Halassa, M.M., Fellin, T., Haydon, P.G.: The tripartite synapse: roles for gliotransmission in health and disease. Trends Mol. Med. **13**, 54–63 (2007). doi:10.1016/j.molmed.2006.12.005
24. Parpura, V., Fang, Y., Basarsky, T., Jahn, R., Haydon, P.G.: Expression of synaptobrevin II, cellubrevin and syntaxin but not SNAP-25 in cultured astrocytes. FEBS Lett. **377**, 489–492 (1995). doi:10.1016/0014-5793(95)01401-2
25. Parpura, V., Liu, F., Brethorst, S., Jeftinija, K., Jeftinija, S., Haydon, P.G.: Alpha-latrotoxin stimulates glutamate release from cortical astrocytes in cell culture. FEBS Lett. **360**, 266–270 (1995). doi:10.1016/0014-5793(95)00121-O
26. Jeftinija, S.D., Jeftinija, K.V., Stefanovic, G.: Cultured astrocytes express proteins involved in vesicular glutamate release. Brain Res. **750**, 41–47 (1997). doi:10.1016/S0006-8993(96)00610-5
27. Calegari, F., Coco, S., Taverna, E., Bassetti, M., Verderio, C., Corradi, N., Matteoli, M., Rosa, P.: A regulated secretory pathway in cultured hippocampal astrocytes. J. Biol. Chem. **274**, 22539–22547 (1999). doi:10.1074/jbc.274.32.22539
28. Zhang, Q., Pangrsic, T., Kreft, M., Krzan, M., Li, N., Sul, J.-Y., Halassa, M., Van Bockstaele, E., Zorec, R., Haydon, P.G.: Fusion related release of glutamate from astrocytes. J. Biol. Chem. **279**, 12724–12733 (2004). doi:10.1074/jbc.M312845200
29. Chen, X., Wang, L., Zhou, Y., Zheng, L.H., Zhou, Z.: "Kiss-and-run" glutamate secretion in cultured and freshly isolated rat hippocampal astrocytes. J. Neurosci. **25**, 9236–9243 (2005). doi:10.1523/JNEUROSCI.1640-05.2005
30. Parri, H.R., Gould, T.M., Crunelli, V.: Spontaneous astrocytic Ca^{2+} oscillations in situ drive NMDAR-mediated neuronal excitation. Nat. Neurosci. **4**, 803–812 (2001). doi:10.1038/90507

31. Fellin, T., Pascual, O., Gobbo, S., Pozzan, T., Haydon, P.G., Carmignoto, G.: Neuronal synchrony mediated by astrocytic glutamate through activation of extrasynaptic NMDA receptors. Neuron **43**, 729–743 (2004). doi:10.1016/j.neuron.2004.08.011
32. Angulo, M.C., Kozlov, A.S., Charpak, S., Audinat, E.: Glutamate released from glial cells synchronizes neuronal activity in the hippocampus. J. Neurosci. **24**, 6920–6927 (2004). doi:10.1523/JNEUROSCI.0473-04.2004
33. Fellin, T., Pozzan, T., Carmignoto, G.: Purinergic receptors mediate two distinct glutamate release pathways in hippocampal astrocytes. J. Biol. Chem. **281**, 4274–4284 (2006). doi:10.1074/jbc.M510679200
34. Newman, E.A.: New roles for astrocytes: regulation of synaptic transmission. Trends Neurosci. **26**, 536–542 (2003). doi:10.1016/S0166-2236(03)00237-6
35. Newman, E.A.: Glial cell inhibition of neurons by release of ATP. J. Neurosci. **23**, 1659–1666 (2003)
36. Di Garbo, A., Barbi, M., Chillemi, S., Alloisio, S., Nobile, M.: Calcium signalling in astrocytes and modulation of neural activity. Biosystems **89**, 74–83 (2007). doi:10.1016/j.biosystems.2006.05.013
37. Höfer, T., Venance, L., Giaume, C.: Control and plasticity of intercellular calcium waves in astrocytes: a modeling approach. J. Neurosci. **22**, 4850–4859 (2002)
38. Putney, J.W., Broad, L.M., Jr., Braun, F., Lievremont, J., Bird, G.J.: Mechanisms of capacitative calcium entry. J. Cell Sci. **114**, 2223–2229 (2001)
39. Targos, B., Barańska, J., Pomorski, P.: Store-operated calcium entry in physiology and pathology of mammalian cells. Acta Biochim. Pol. **52**, 397–409 (2005)
40. Randriamampita, C., Tsien, R.Y.: Emptying of intracellular Ca^{2+} stores releases a novel small messenger that stimulates Ca^{2+} influx. Nature **364**, 809–814 (1993). doi:10.1038/364809a0
41. Berridge, M.J.: Capacitative calcium entry. Biochem. J. **312**, 1–11 (1995)
42. Volterra, A., Steinhauser, C.: Glial modulation of synaptic transmission in the hippocampus. Glia **47**, 249–257 (2004). doi:10.1002/glia.20080
43. North, R.A., Barnard, E.A.: Nucleotide receptors. Curr. Opin. Neurobiol. **7**, 346–357 (1997). doi:10.1016/S0959-4388(97)80062-1
44. Khakh, B.S., Gittermann, D., Cockayne, D.A., Jones, A.: ATP modulation of excitatory synapses onto interneurons. J. Neurosci. **23**, 7426–7437 (2003)
45. Bowser, D.N., Khakh, B.S.: ATP excites interneurons and astrocytes to increase synaptic inhibition in neuronal networks. J. Neurosci. **24**, 8606–8620 (2004). doi:10.1523/JNEUROSCI.2660-04.2004
46. Kawamura, M., Gachet, C., Inoue, K., Kato, F.: Direct excitation of inhibitory interneurons by extracellular ATP mediated by P2Y receptors in the hippocampal slice. J. Neurosci. **24**, 10835–10845 (2004). doi:10.1523/JNEUROSCI.3028-04.2004
47. Fries, P., Nikolik, D., Singer, W.: The gamma cycle. Trends Neurosci. **30**, 309–316 (2007). doi:10.1016/j.tins.2007.05.005
48. Freund, T.F.: Interneuron diversity series: rhythm and mood perisomatic inhibition. Trends Neurosci. **26**, 489–495 (2003). doi:10.1016/S0166-2236(03)00227-3
49. Hestrin, S., Galarreta, M.: Electrical synapses define networks of neocortical GABAergic neurons. Trends Neurosci. **28**, 304–309 (2005). doi:10.1016/j.tins.2005.04.001
50. Mann, E.O., Paulsen, O.: Role of GABAergic inhibition in hippocampal network oscillations. Trends Cogn. Sci. **30**, 343–349 (2007)
51. Nadkarni, S., Jung, P.: Spontaneous oscillations of dressed neurons: a new mechanism for epilepsy? Phys. Rev. Lett. **91**, 268101(4) (2003)
52. Nadkarni, S., Jung, P.: Dressed neurons: modelling neural–glia interactions. Phys. Biol. **1**, 35–41 (2004). doi:10.1088/1478-3967/1/1/004
53. Olufsen, M., Whittington, M., Camperi, M., Kopell, N.: New roles for the gamma rhythm: population tuning and preprocessing for the beta rhythm. J. Comput. Neurosci. **14**, 33–54 (2003). doi:10.1023/A:1021124317706
54. Sneyd, J., Tsaneva-Atanasova, K., Yule, D.I., Thompson, J.L., Shuttleworth, T.J.: Control of calcium oscillations by membrane fluxes. Proc. Natl. Acad. Sci. U. S. A. **101**, 1392–1396 (2004). doi:10.1073/pnas.0303472101
55. Lavrentovich, M., Hemkin, S.: A mathematical model of spontaneous calcium (II) oscillations in astrocytes. J. Theor. Biol. **251**, 553–560 (2008). doi:10.1016/j.jtbi.2007.12.011
56. Parri, H.R., Crunelli, V.: The role of Ca^{2+} in the generation of spontaneous astrocytic Ca^{2+} oscillations. Neuroscience **120**, 979–992 (2003). doi:10.1016/S0306-4522(03)00379-8
57. Aguado, F., Espinosa-Parrilla, J.F., Carmona, M.A., Soriano, E.: Neuronal activity regulates correlated network properties of spontaneous calcium transients in astrocytes in situ. J. Neurosci. **22**, 9430–9444 (2002)

58. Tashiro, A., Goldberg, J., Yuste, R.: Calcium oscillations in neocortical astrocytes under epileptiform conditions. J. Neurobiol. **50**, 45–55 (2002). doi:10.1002/neu.10019
59. Nett, W., Oloff, S.H., McCarthy, K.D.: Hippocampal astrocytes in situ exhibit calcium oscillations that occur independent of neuronal activity. J. Neurophysiol. **87**, 528–537 (2002)
60. Egan, T.M., Samways, D.S.K., Li, Z.: Biophysics of P2X receptors. Pflugers Arch. Eur. J. Physiol. **452**, 501–512 (2006)
61. Li, X.Y., Rinzel, J.: Equations of IP3 receptor-mediated Ca^{2+} oscillations derived from a detailed kinetic model: a Hodgkin-Huxley like formalism. J. Theor. Biol. **166**, 461–473 (1994). doi:10.1006/jtbi.1994.1041